Devitrification of glassy $Al_{85}Ni_{10}La_5$ powder by Thermal Treatment and Ball-Milling

Yao Liu, Gerhard Schumacher, Sören Zimmermann and John Banhart

Helmholtz-Zentrum Berlin für Materialien und Energie, Hahn-Meitner-Platz 1, D-14109 Berlin, Germany

Abstract

Structural stability of glassy $Al_{85}Ni_{10}La_5$ as-atomized powder was investigated after ball-milling using differential scanning calorimetry, X-ray diffractometry, and transmission electron microscopy. Fcc-Al nanocrystals were found after ball-milling. The crystallization behavior upon thermal treatment depends on the deformation level. This is ascribed to a shift in the composition of the residual amorphous phase towards higher contents of Ni and La during ball-milling.

Keywords: Ball-milling, Aluminium alloy, plastic deformation, crystallization, amorphous alloy

Introduction

Al-based amorphous alloys with Al concentrations of 80-90 at% have attracted much attention due to their mechanical properties, especially the high strength combined with a good ductility which is superior to that of conventional high-strength aluminum alloys [1, 2]. The mechanical properties of partially crystallized amorphous alloys with nanometer-sized Al crystals could be even improved [3, 4]. For Al-RE-TM type amorphous alloys (RE: rare earth elements, TM: transition metals) with amorphous/nanocrystalline composite microstructure the strength was shown to increase up to 1560 MPa [5]. The nanocrystals can be produced either by heat treatment [6] or by plastic deformation [7-13], e.g., cold rolling [7], nanoindentation [8], high pressure torsion [9], equal channel angular pressing [10] ball-milling [11] and extreme bending [12, 13]. It is yet unclear whether the underlying mechanism for stress-induced crystallization is thermal or athermal.

This work reports the structural changes of helium-atomized $Al_{85}Ni_{10}La_5$ amorphous powder during plastic deformation by ball-milling at different temperatures. The structural changes are compared to those observed after thermal treatment.

Experimental

The alloy with nominal composition $Al_{85}Ni_{10}La_5$ was synthesized in an alumina crucible by induction melting under argon atmosphere, using pure elements of Al (99.98%), Ni (99.7%) and La (99.7%). The melt was heated up to approximately 1200°C and was subsequently atomized by Nanoval G.m.b.H. using the "Nanoval" process [14]

and helium gas. The plastic deformation of as-atomized powder was performed by ball-milling at three different temperature ranges (-80°C < T < -50°C; room temperature; 80°C < T < 100°C) using a Spex Mixer Mill 8000. Six samples were prepared using different ball-milling times of 60min, 120min, 240min, 600min, 1200min and 6000min.

Differential scanning calorimetry (DSC) was carried out in a Perkin-Elmer Pyris-1 under a stream of argon gas during continuous heating at different heating rates ranging from 5K/min to 80K/min. After the first run on the as-atomized or ball-milled powder, the sample was cooled down to 50 °C and then heated up again with the same heating rate. The second run in which the sample was already fully crystalline served as the baseline which was subtracted from the corresponding first-run data. Kissinger analysis was applied to determine the activation energies of phase transformations in the as-atomized and ball-milled powders.

Scanning electron microscopy (SEM) was done using a Zeiss 1540EsB CrossBeam® workstation containing an ultra-high resolution GEMINI® field emission column. The structure of the powders was proven by X-ray diffraction (XRD) in a Bruker D8 Advance diffractometer using Cu K_α radiation. The software "X'Pert HighScore Plus" was used to determine the crystallite size from the XRD patterns. Transmission electron microscopy (TEM) was done in a Philips CM 30 microscope operated at 300kV. The amorphous nature of the material was confirmed by TEM bright field microscopy and by selected-area electron diffraction.

Results and discussion

The microstructures of the powder particles in the as-atomized state and after ball-milling to 1200 min are shown in Fig. 1a and Fig. 1b, respectively. The powder particles in the as-atomized state have a spherical shape and a smooth surface. Small particles of the order of 0.2 μm in size are attached to the surface of powder particles with particle diameter of several μm. The mean particle diameter was determined to d = (11 ± 1) μm [10]. During ball-milling, the size and shape of the particles changes drastically. The particle size was found to increase during ball milling to 1200 min by about one order of magnitude followed by a decrease in particle size on subsequent milling (not shown here). Furthermore, the surface of the particles has got rough compared to the as-atomized particles pointing to severe plastic deformation of the individual particles joint together by a cold welding process during ball-milling explaining the increase in particle size. The decrease in particle size beyond 1200 min is ascribed to embrittlement due to the precipitation of fcc-Al nanocrystals and the related change in composition of the residual amorphous matrix.

The DSC signal measured during continuous heating of the powder in the as-atomized state and after ball-milling at room temperature to different times using a heating rate of 20K/min is shown in Fig. 2. The DSC curve of the as-atomized powder reveals a pronounced glass transition at T_g = 253.5°C (T_g: glass transition temperature). The pronounced glass transition points to the glassy nature of the as-atomized material. The DSC trace above T_g can be fitted by two Gaussians and two asymmetric double sigmoidal

functions indicating four exothermal reactions, see inset of Fig. 2. XRD analyses of powders heated to different temperatures showed that the first exothermal peak can be assigned to the precipitation of fcc-Al, the second to a metastable phase formation, the third and the fourth to Al_3Ni and $Al_{11}La_3$ (results not shown here). As a function of the ball-milling time the glass transition vanishes. This disappearance in the glass transition might be due to a fragile-to-amorphous transition in accordance to Louzguine et al. [15] who observed the disappearance of a glass transition in Al-Y-Ni-Co-Sc glasses with increase of the Sc content.

The heat release of the first and second exothermal reactions decreases with increasing ball-milling time and completely vanished after ball-milling to 6000 min while the third and fourth peak increased. This is ascribed to the deformation-induced precipitation of fcc-Al crystals and the related change in composition of the residual amorphous phase which crystallizes differently from the as-sprayed powder. The energy gain due to the transformation from the metastable phase to the final crystallization products Al_3Ni and $Al_{11}La_3$ is obviously lower than the gain from the amorphous phase to the final products.

The peak temperature T_p at which the maximum heat release occurred in the DSC curves changes with heating rate. Thus, the activation energy E related to the crystallization of the fcc-Al was deduced directly from the values of T_p of the first exothermal reaction by Kissinger analysis [16] shown in Table 1. The activation energy for the precipitation of fcc-Al was found to decrease from 295 kJ/mol for the as-atomized powder to 240 kJ/mol for the specimen ball-milled to 6000 min. This decrease in activation energy indicates a decrease in the stability of the amorphous phase.

In order to assign the exothermal reactions to crystallization products we performed XRD measurements after each of the ball-milling times. The XRD patterns of the material in the as-atomized state and after different ball-milling times are shown in Fig. 3. The XRD pattern of the as-atomized material reveals a broad maximum at $2\Theta \approx 37°$ with a shoulder at $2\Theta \approx 44°$ pointing to an amorphous structure. We fitted the spectrum of the as-atomized powder by two Gaussian functions according to Louzguine and Inoue [17] and deduced from the fit to the shoulder a coherency length of 1.9 nm by the use of Scherrer's equation. The coherency length of the X-rays is assigned to nuclei of fcc crystals. Nanocrystals of about the same size have been found in several Al-based amorphous alloys. Strunz and coworkers detected heterogeneities with size of 1.1 nm in amorphous powders of the same alloy [18]. Sahoo and coworkers [19] found nanocrystals smaller 2 nm in size in amorphous $Al_{89}Ni_6La_5$ alloy by means of small angel neutron scattering (SANS). Louzguine and Inoue [17] deduced from the shoulders in the X-ray spectra of their Al-based amorphous materials fcc-Al nanocrystals of 2.5 - 2.7 nm in size.

The XRD pattern of the powder ball-milled to 1200 min reveals reflections of low intensity at $2\Theta = 38.5°$ and $2\Theta = 44.8°$ which we assigned to the 111 and 200 reflections, respectively, of the fcc-Al phase. The intensity of these peaks increased during ball-milling to 6000 min. Furthermore, reflections at $2\Theta = 65.3°$ and $2\Theta = 78.5°$ are now clearly visible. These maxima are assigned to the 220 and 311 reflections of the fcc-Al phase. This is in qualitative agreement with the results obtained after high pressure

torsion of the same powder where fcc nanocrystals have been detected by means of energy dispersive diffraction of X-rays [9]. The size of the Al-nanocrystals was determined by fitting a Gaussian to the 111- and 200-reflections and by the use of Scherrer's equation taking into account the intrinsic line width. The crystallite size of the specimen ball-milled to 1200 min is 11 ± 1 nm while the size of the specimen ball-milled to 6000 min is 12 ± 1 nm. Within the experimental uncertainty the crystallite size is therefore the same for the two milling times while the volume amount increases from 2.6% to 6.1 % by increasing the milling time from 1200 min. to 6000 min. It is generally accepted that formation of fcc-Al nanocrystals during plastic deformation occurs in or close to shear bands which typically have a thickness of ~10 nm. The distance between shear bands after simple deformation is of the order of ~1μm [2]. The high volume fraction (6.1%) of Al nanocrystals in the specimen ball-milled to 6000 min therefore suggests a large volume fraction of shear bands produced due to multiple deformations during long ball-milling times. The reasons for the weak dependence of nanocrystal size on deformation level is not quite clear. It might be the result of a fragmentation mechanism acting at high deformation levels as proposed in [20].

Fig. 4 shows the XRD pattern of as-atomized powder and of powder ball-milled to 600min and 1200min thermally treated to 300 °C with 20 K/min. The maxima in the intensities of the as-atomized powder can be indexed by the reflections of fcc-Al and by the maxima of an unknown metastable phase. Ball-milling to 600 min leads to a relative decrease of the maxima of the metastable phase which completely vanish after ball-milling to 1200min. This leads to the conclusion that plastic deformation by ball-milling leads to a change in the crystallization behavior due to a shift of the composition of the residual amorphous matrix caused by the precipitation of fcc-Al.

Ball-milling at temperatures between 80°C and 100°C for 240 min leads to an enhanced precipitation of fcc-Al nanocrystals compared to ball-milling at room temperature while ball-milling at temperatures between -80°C and -50°C for 240 min hardly leads to the formation of fcc-Al precipitates (see Fig. 5). Though all of the ambient temperatures are far below the crystallization temperature, the precipitation process is affected in a way that higher temperatures enhance crystallization while lower temperatures hamper crystallization of fcc-Al nanocrystals. Our results therefore suggest a combined influence of temperature and plastic deformation on crystallization. This interpretation is in qualitative agreement with the finding of Lee et al. [21] who studied the influence of uniaxial pressure and plastic deformation of a Cu metallic glass. They found that hydrostatic pressure reduces the activation energy for nucleation while the shear stress lowers the activation energy for the diffusion of a matrix atom to the nucleus. In ball-milling experiments both hydrostatic pressure and shear stresses act to the powder particles [22]. We therefore conclude that the activation energies for nucleation and growth during ball-milling of $Al_{85}Ni_{10}La_5$ powder also decrease resulting in deformation induced precipitation of fcc-Al in amorphous Al-based matrix.

The influence of temperature on the precipitation of fcc-Al is also reflected in the DSC curves measured after ball milling to 120 min at different temperatures (see Fig. 6). First, the heat release assigned to the precipitation of Al-fcc nanocrystals decreases with

increasing ball-milling temperature. This means that the volume fraction of fcc-Al nanocrystals increases with increasing ball-milling temperature in agreement with the results from XRD measurements (see Fig. 5). Furthermore, the glass transition is reduced with increasing ball-milling temperature.

Summary and Conclusions

Structural stability of $Al_{85}Ni_{10}La_5$ as-atomized powder was investigated in the as-atomized condition and after ball-milling using different methods like differential scanning calorimetry, X-ray diffractometry, and transmission electron microscopy. Thermal treatment of as-atomized powder to 300°C causes the formation of fcc-Al and a metastable phase, while thermal treatment of powders ball-milled to times larger than 1200 min yields in the formation of fcc-Al only indicating the destruction of the metastable phase by plastic deformation and/or a shift in the composition of the residual amorphous phase towards higher contents of Ni and La. The formation of fcc-Al nanocrystals and the destruction of the metastable phase during ball-milling cause a gradual change of the DSC diagram. The decrease in activation energy and the gradual vanishing of the glass transition with increasing ball-milling time indicate a decrease in the stability of the residual amorphous matrix and, possibly, a fragile-strong glass transition.

References

[1] A. Inoue, K.Ohtera, A. P.Tsai, and T. Masumoto, Jpn. J. Appl.Phys, 276 (1988) L280.

[2] Y.He,S. J. Poon, and G. J. shiflet, Science 241, (1988)1640.

[3] H.Chen,Y.He,G.J. Shiflet, and S. J. Poon, Scr. Metall. Mater. 25, (1991) 1421.

[4] A. Inoue, Prog. Mater. Sci. 43, (1998) 365.

[5] Y.H. Kim, A. Inoue, T. Masumoto, Mater. Trans. JIM 31 (1990) 747.

[6] A. P. Tsai, T. Kamiyama, Y.Kawamura, A. Inous, T. Masumoto, Acta Mater.45 (1997) 1477.

[7] J. H. Perepezko, R. J. Hebert, R. I. Wu, Mater. Sci. Forum 386-388 (2002) 11

[8] J. J. Kim, Y. Choi, S. Suresh, A. S. Argon, Science 295 (2002) 654

[9] J. Vierke, G. Schumacher, V. P. Pilyugin, I. A. Denks, I. Zizak, C. Wolf, N. Wanderka, M. Wollgarten, J. Banhart, J. Alloys and Comp. 493 (2010) 683.

[10] J. Vierke, PhD, Technische Universität Berlin (2008).

[11] Z. Zhang, Y. Zhou, E. J. Lavernia Alloys and Comp. 466 (2008) 189.

[12] W.H, Jiang, F.E. Pinkerton, M. Atzmon, Scripta Mater. 48 (2003) 1195

[13] H. Chen, Y. He, G.J. Shiflet, S.J.Poon, Nature 367 (1994) 541

[14] L.Gerking, Powder Metall.Int.25 (1993)59.

[15] D. V. Louzguine-Luzgin, S. Sobu and A. Inoue, Appl. Phys. Lett. 85 (2004) 3758.

[16] H. E. Kissinger, J. Res. Natl. Bureau Stand. 57 (1956) 217.

[17] D. V. Louzguine-Luzgin, A. Inoue, J. Alloys and Comp. 399 (2005) 78.

[18] P. Strunz, Y. Liu, G. Schumacher, V. Ryutkin, U. Keiderling, unpublished results

[19] K.L.Sahoo, M.Wollgarten, J. Haug, J.Banhart, Acta. Mater. 53(2005) 3861.

[20] R.J. Hebert, J.H. Perepezko, H. Rösner and G. Wilde, Scripta Mater 54 (2006) 25.

[21] S.-W. Lee, M.-Y. Huh, S.-W. Chae, J.-C. Lee, Scripta Materialia 54 (2006) 1439.
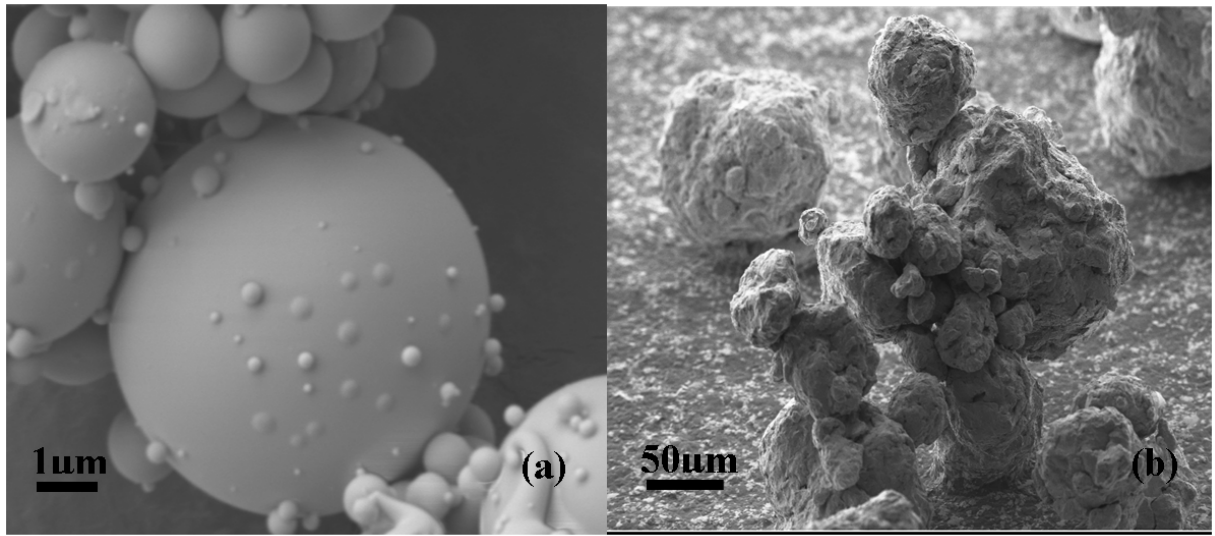
[22] C. Suryanarayana, Prog. Mater. Sci. 46 (2001)

Fig. 1: scanning electron micrograph of $Al_{85}Ni_{10}La_5$ in the as-atomized condition (a) and after ball-milling to 1200 min. (b).
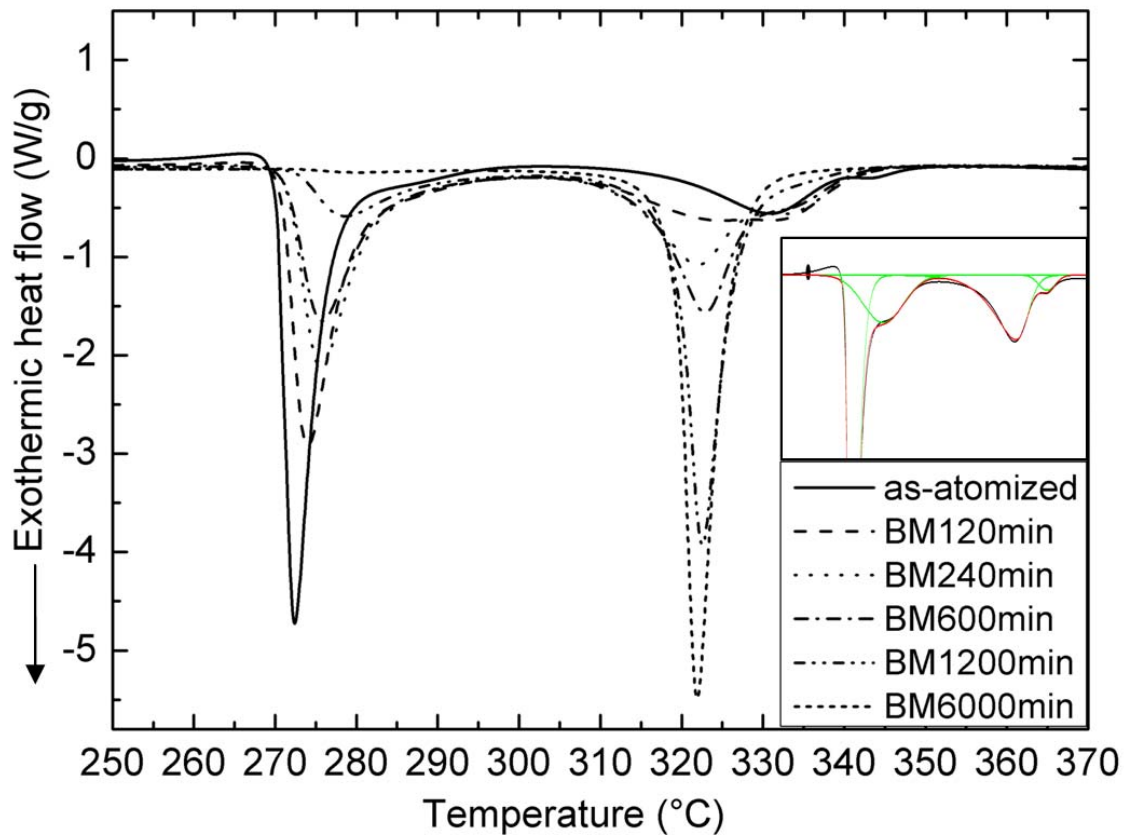
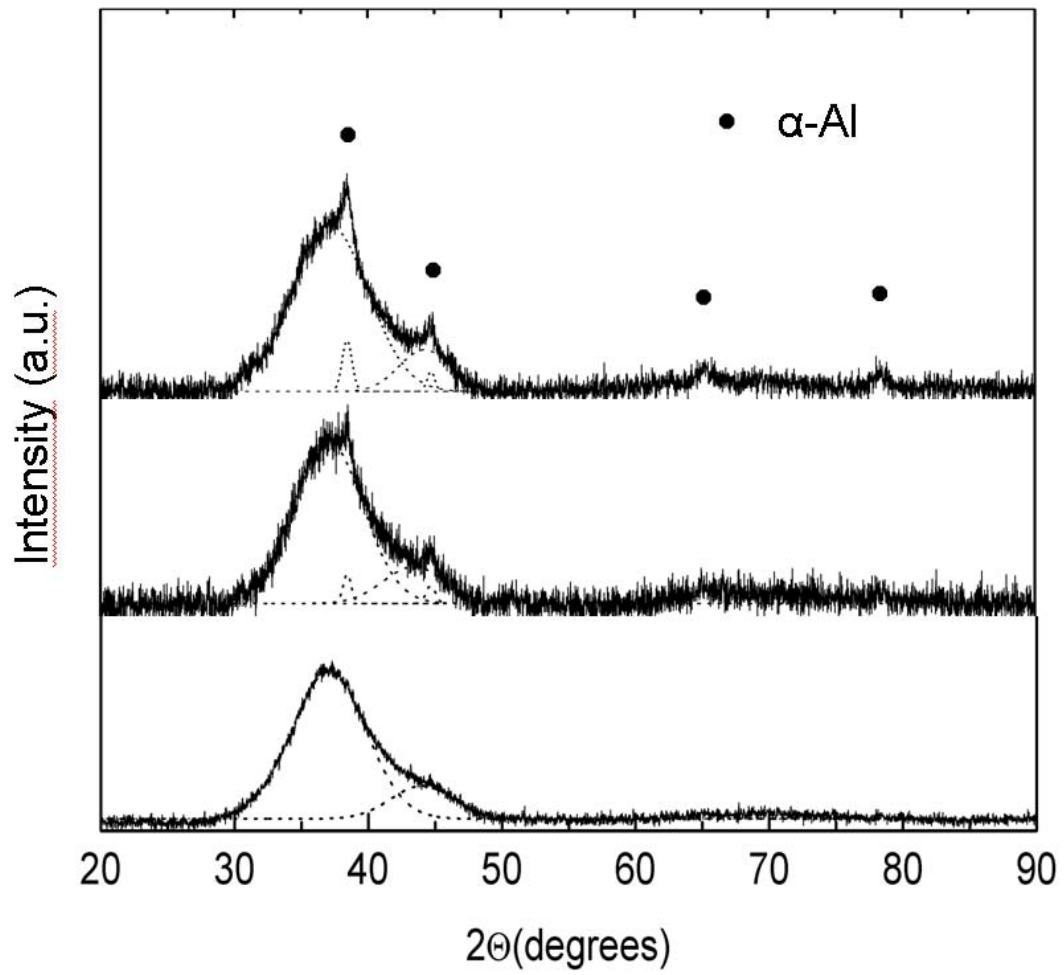Fig. 2: DSC curves of $Al_{85}Ni_{10}La_5$ powders ball-milled at room temperature to different times.

Fig. 3: XRD pattern of $Al_{85}Ni_{10}La_5$ powder in as-atomized condition (bottom), after ball-milling to 1200 min (middle) and after ball-milling to 6000 min.

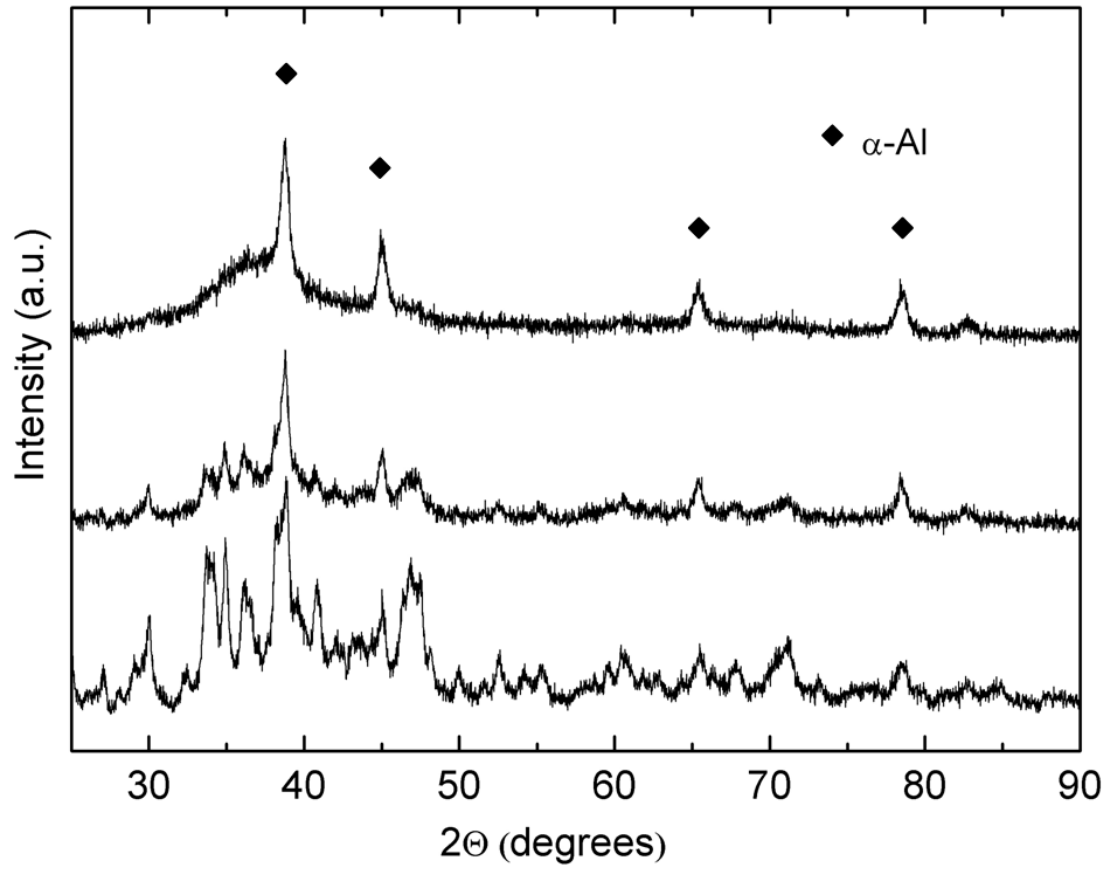Fig. 4: XRD pattern of $Al_{85}Ni_{10}La_5$ powder in the as-atomized condition (bottom), after ball-milling to 600 min (middle), and after ball-milling to 1200 min (top), each after additional annealing to 300°C.
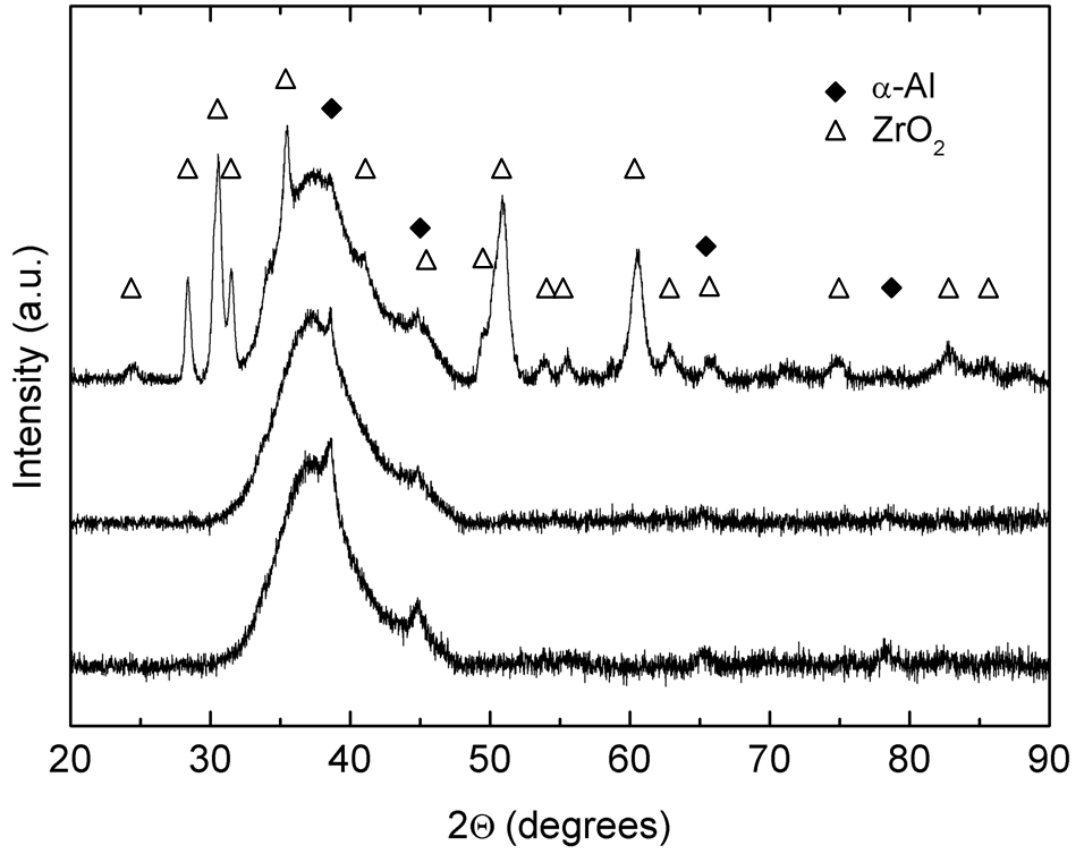
Fig. 5: XRD pattern of $Al_{85}Ni_{10}La_5$ powder ball-milled to 240 min at low temperature (-80°C < T < -50°C, top), at room temperature (middle), and at high temperature (80°C < T < 100°C, bottom). The peaks marked by triangles are due to ZrO_2 weared from the container and the balls during low temperature milling.
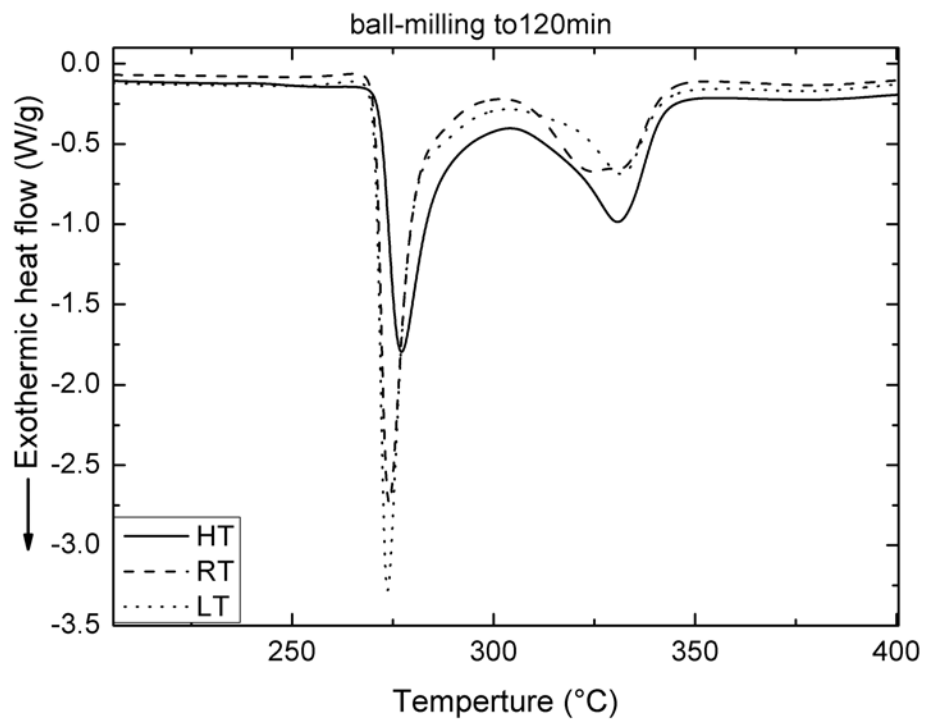
Fig. 6: DSC curves of $Al_{85}Ni_{10}La_5$ powders ball-milled at high temperature (HT), room temperature (RT) and low temperature (LT) to 120min.

Table1: Activation energy of crystallization of $Al_{85}Ni_{10}La_5$ powder ball-milled to different times.

	E (kJ/mol)
As-atomized	295±11
BM 30min	275±14
BM 60min	286±11
BM 240min	276±13
BM 600min	248±14
BM 1200min	240±13